Cellular Signalling 56 (2019) 1–14

Contents lists available at ScienceDirect

Cellular Signalling

journal homepage: www.elsevier.com/locate/cellsig

Low expression of PDK1 inhibits renal cell carcinoma cell proliferation, migration, invasion and epithelial mesenchymal transition through inhibition of the PI3K-PDK1-Akt pathway

Wei-Min Zhou[a,b], Gao-Liang Wu[b], Ji Huang[b], Jin-Gao Li[c], Chao Hao[b], Qiu-Ming He[b], Xiao-Dan Chen[d], Gong-Xian Wang[a,e,*], Xin-Hua Tu[b,**]

[a] Jiangxi Medical College, Nanchang University, Nanchang 330006, PR China
[b] Department of Urology, Jiangxi Cancer Hospital, Nanchang 330029, PR China
[c] Department of Radiotherapy, Jiangxi Cancer Hospital, Nanchang 330029, PR China
[d] Department of Science and Education, Jiangxi Cancer Hospital, Nanchang 330029, PR China
[e] Department of Urology, The First Affiliated Hospital of Nanchang University, Nanchang 330006, PR China

ARTICLE INFO

Keywords:
Renal cell carcinoma
PDK1
Epithelial mesenchymal transition
PI3K-PDK1-Akt pathway
Proliferation
Migration
Invasion

ABSTRACT

As the most commonly occurring form of primary renal tumor, renal cell carcinoma (RCC) is a malignancy accompanied by a high mortality rate. 3-phosphoinositide-dependent protein kinase 1 (PDK1) has been established as a protein target and generated considerable interest in both the pharmaceutical and academia industry. The aim of the current study was to investigate the effect of si-PDK1 on the RCC cell apoptosis, proliferation, migration, invasion and epithelial mesenchymal transition (EMT) in connection with the PI3K-PDK1-Akt pathway. Microarray analysis from the GEO database was adopted to identify differentially expressed genes (DEGs) related to RCC, after which the positive expression of the PDK1 protein in tissue was determined accordingly. The optimal silencing si-RNA was subsequently selected and RCC cell lines 786-O and A498 were selected and transfected with either a si-PDK1 or activator of the PI3K-PDK1-Akt pathway for grouping purposes. The mRNA and protein expressions of PDK1, the PI3K-PDK1-Akt pathway-, EMT- and apoptosis-related genes were then evaluated. The effect of si-PDK1 on cell proliferation, apoptosis, invasion and migration was then analyzed. Through microarray analysis of GSE6344, GSE53757, GSE14762 and GSE781, PDK1 was examined. PDK1 was determined to be highly expressed in RCC tissues. Si-PDK1 exhibited marked reductions in relation to the mRNA and protein expression of PDK1, PI3K, AKT as well as Vimentin while elevated mRNA and protein expressions of E-cadherin were detected, which ultimately suggested that cell migration, proliferation and invasion had been inhibited coupled with enhanced levels of cell apoptosis. While a notable observation was made highlighting that the PI3K-PDK1-Akt pathway antagonized the effect of PDK1 silencing. Taken together, the key observations of this study provide evidence suggesting that high expressions of PDK1 are found in RCC, while highlighting that silencing PDK1 could inhibit RCC cell proliferation, migration, invasion and EMT by repressing the PI3K-PDK1-Akt pathway.

1. Introduction

Renal cell carcinoma (RCC) represents the most prevalent kidney tumor, representing approximately 3% of all adult advanced tumors [1]. RCC is characterized by > 10 molecular and histological subtypes, among which clear cell RCC (ccRCC) is the most commonly occurring

Abbreviations: RCC, renal cell carcinoma; PDK1, 3-phosphoinositide-dependent protein kinase 1; EMT, epithelial mesenchymal transition; GEO, Gene Expression Omnibus; RMA, robust multiarray average; TNM, tumor node metastasis; PBS, phosphate buffered saline; RPMI, Royal Park Memorial Institute; BCA, bicinchoninic acid; SDS-PAGE, sodium dodecyl sulfate polyacrylamide gel electrophoresis; PVDF, polyvinylidene fluoride; HRP, horseradish peroxidase; BSA, bovine serum albumin

* Correspondence to: Gong-Xian Wang, Jiangxi Medical College, Nanchang University, No. 461, Bayi Avenue, East Lake District, Nanchang 330006, Jiangxi Province, PR China.
** Correspondence to: Xin-Hua Tu, Department of Urology, Jiangxi Cancer Hospital, No. 519, Beijing East Road, Qingshan Lake District, Nanchang 330029, Jiangxi Province, PR China.
E-mail addresses: gongxianwang118@163.com (G.-X. Wang), tu_xinhua@126.com (X.-H. Tu).

https://doi.org/10.1016/j.cellsig.2018.11.016
Received 11 July 2018; Received in revised form 16 November 2018; Accepted 19 November 2018
Available online 20 November 2018
0898-6568/

accounting for 70% of all diagnosed cases [2]. Reports have indicated that RCC develops in a slower more progressive manner, with some long-term cases largely asymptomatic which may spread to the lymph nodes, lung, liver and bone in the majority of cases [3]. However, as one of the most fatal urological tumors in the world, RCC's early clinical manifestation is largely nonspecific, which often results in diagnosis at late stages [4]. Although typical treatment methods, including chemotherapy, hormone therapy, and radiotherapy, have all been shown to improve the overall survival rate of patients with RCC [5], approximately 20–40% patients run the risk of recurrence post surgery [1]. Epithelial mesenchymal transition (EMT) is a crucial element in the event of distant metastasis and cancer recurrence [6]. The limited molecular driving force of RCC leads to a general overall lack of efficient treatment for patients who suffer from this progressive disease [4].

3-phosphoinositide-dependent protein kinase 1 (PDK1), is a key regulator of cell migration and chemotaxis and elicits is functions through various components of signal transduction and cytoskeletal dynamics, which have been reported to exhibit significant functions in regulating migration in different kinds of epithelial cells [7]. As one of the most important pathways, PI3K/Akt mediated signal transduction possesses the ability to regulate metabolism, proliferation as well as the survival of mammalian cells [8]. The PI3K/Akt pathway has been linked with Insulin-like Growth Factors-1 (IGF-1)-induced cell survival, with certain reports suggesting that the Akt pathway could be regulated by PDK1 [9]. Cell survival and growth have been shown to be significantly influenced through the AKT/PDK1 pathway *via* various mechanisms [10]. The expressions of phospho-PI3K, phospho-PDK1 and phospho-AKT in RCC were significantly decreased by Tetrandrine (Tet), while the phosphorylation of Akt has been highlighted as the responsible factor regarding the anti-metastatic effects in RCC induced by Tet [11]. Tet is a bisbenzylisoquinoline alkaloid employed in the treatment of hypertension, arrhythmic and rheumatism, exhibiting cancer-suppressive powers in different kinds of cancers and acting to inhibit growth and angiogenesis while elevating cancer apoptosis [11]. Although evidence has been provided highlighting the means by which the PI3K/PDK1/Akt pathway is inhibited to restrain the abnormal motility and proliferation of lung epithelial cells [12], there is a scarcity of information regarding the connection between PDK1, the PI3K/PDK1/Akt pathway and RCC. Hence the present study was performed to validate the effect of siRNA-mediated silencing of PDK1 on the proliferation, apoptosis and EMT of RCC cells with the involvement of the PI3K/PDK1/Akt pathway.

2. Materials and methods

2.1. Ethics statements

The study was conducted with the approval of the clinical laboratory ethics committee of Jiangxi Cancer Hospital. All participating patients and their families singed informed consent documentation prior to being enrolled into the study prior to specimen collection. The experiment was performed in strict adherence with the *Helsinki declaration*.

2.2. Microarray data analysis

The Gene Expression Omnibus (GEO) database was employed in order to retrieve the gene expression chip of RCC using “Renal Cell Carcinoma” as the key word, “Expression profiling by array” as type and “*Homo sapiens*” as organism to screen out data expression chips that contained RCC tissues and adjacent normal tissues. Finally, GSE6344, GSE53757, GSE14762 and GSE781 were selected for further analysis. The robust multiarray average (RMA) algorithm [13] in R language Affy package (http://www.bioconductor.org/packages/release/bioc/html/affy.html) was employed in the process of standardizing the chip expression data. The *t*-test of limma package (http://master.bioconductor.org/packages/release/bioc/html/limma.html) in R software was used to identify the differentially expressed genes (DEGs) between RCC tissue and adjacent normal tissues. Genes with $|\text{LogFoldChange}| > 2.0$ and $p < 0.05$ were identified as the significantly differentially expressed. The heat map of the DEGs was drawn, and the Venn on-line analysis tool Calculate and draw custom Venn diagrams (http://bioinformatics.psb.ugent.be/webtools/Venn/) was applied for comparison of DEGs in the 4 chips. Genes related to RCC were retrieved in DisGeNET database (http://www.disgenet.org/web/DisGeNET/menu/search? 4) which provided data pertaining to the links between a large number of genes and diseases [14]. The Search Tool for the Retrieval of Interacting Genes (STRING) (http://www.string-db.org/), is a protein synthesis information online database, and the STRING tool was adopted in order to analyze the interaction between DEGs and disease-related genes. The confidence score > 0.4 was set when the interaction relationship was predicted, and the gene interaction network was visualized in the Cytoscape 3.6.0 software [15].

2.3. Study subjects

A total of 112 patients (67 female and 45 male patients aged between 28 and 66 years and with a mean age of 49.2 years) with RCC accepting surgical excision at Jiangxi Cancer Hospital were selected for sample collection. The tissue samples were fixed in 10% formalin solution, embedded in paraffin, then cut into 4 μm slices, and stored at −80 °C. Among the 112 patients, there were 62 cases of lymph node metastasis and 50 cases free of lymph node metastasis; 18 cases were confirmed to be at stage I, 59 cases at stage II, 35 cases at stage III in accordance with the WHO/ISUP grading system [16]; according to tumor node metastasis (TNM) staging system [17], 26 cases were confirmed to be at stage I/II, and 86 cases at stage III/IV. There were 58 cases with tumor diameter over or equal to 7 cm and 54 cases < 7 cm. Patient inclusion criteria were as follows: [18] patients with RCC were verified *via* CT scanning by a 64 bit sensor (Siemens, Erlangen, Germany) [19], including clear cell RCC, papillary RCC, and eosinophilic RCC; patients were yet to receive radiochemotherapy; patients free of any systemic disease; patients with TNM classification including stage I, II, III, and IV. Patient exclusion criteria: mental disorders and unable to communicate; patients had other tumor disease or tumor history; alcoholic and drug abusers; patients had undergone operations like gynecologic surgical procedures and cholecystectomy during the RCC operation.

2.4. Immunohistochemistry

The tissues embedded in paraffin were cut into sections, then orderly placed in dimethylbenzene solution and immersed for 15 min, after which dimethylbenzene was replaced. The sections were hydrated with absolute alcohol for 5 min and then rehydrated for 5 min with replaced absolute alcohol. Afterwards, the sections were hydrated in a successive fashion with 70% and 95% alcohol respectively for 10 min. Each section was then added with 3% H_2O_2 solution and was placed at room temperature for 10 min for blockade with endogenous peroxidase. After the addition of citric acid buffer and incubation in a microwave oven for 3 min, antigen retrieval buffer was added to the sections and placed at room temperature for 10 min. The sections were then washed three times with phosphate buffered saline (PBS). Normal goat serum blocking solution (Shanghai Sangon Biological Engineering Co., Ltd., Shanghai, China) was added to the sections at room temperature for 20 min. The sections were then added with diluted rat anti-PDK1 polyclonal antibody (1: 500, ab110025, Abcam, Cambridge, UK) overnight at 4 °C after which they were washed three times with PBS. The sections were then incubated with biotin-labeled goat anti-mouse IgG secondary antibody (1: 200, A21210, AmyJet Scientific Inc., Wuhan, Hubei, China) for 30 min, added with Strept Avidin-Biotin

Complex (SABC) (Vector Laboratories, Inc., Burlingame, CA, USA) and allowed to rest in an incubator at 37 °C for 30 min. The sections were respectively developed for 6 min with one drop of developing solution A, B, C of diaminobenzidine (DAB) Assay Kit (Sigma-Aldrich Chemical Company, St Louis, MO, USA). Next, the sections were stained with hematoxylin for 30 s and dehydrated with 70%, 80%, 90%, 95% and absolute alcohol for 2 min each time. The dimethylbenzene was used to clear the sections twice (5 min each time) with neutral resin employed for sealing purposes. Finally, PBS solution replaced the primary antibody and was regarded as the negative control. The sections were observed and recorded under the microscope (Olympus Optical Co., Ltd., Tokyo, Japan). Yellowish-brown in the cytoplasm was identified as positive staining. Positive cells were averaged by randomly selecting five high power visual fields under a 10 × 40 times light microscope (100 cells were counted in each field). Finally, the total percentage of positive cells to total cells was calculated and considered to be reflective of the positive expression rate. The clinical results from RCC patients were judged by H-score, using the total number of positive cells and the degree of staining: H-score = π (i + 1), i represented the degree of staining (0, 1, 2, 3, 4), while π was reflective of the percentage of cells that expressed various colors (ranging from 0–100%). The expression of PDK1 during our study was defined as high expression when H-score score was over 100%, while low expression was considered to be equal or < 100%.

2.5. Cell culture

RCC cell lines A498 [American Type Culture Collection (ATCC)] and 786-O (Wuhan Boster Biological Technology Co., Ltd., Wuhan, Hubei, China) were selected for cell culture. The 786-O cell line was removed from the liquid nitrogen tank followed by prompt water bating at 37 °C in order to melt the freezing medium within 1 min by means of repeated oscillation. The cells were removed under sterile conditions, with the cell suspension then transferred into a centrifuge tube, slowly added with 2 mL fresh Royal Park Memorial Institute (RPMI) 1640 medium containing 10% fetal bovine serum (FBS) (Shanghai Sangon Biological Engineering Co., Ltd., Shanghai, China). The cell suspension was subsequently centrifuged, re-suspended with culture medium, and repeatedly triturated. The cells were then cultured in a 5% CO_2 incubator at 37 °C and sub-cultured after growing into a compact monolayer. Then cells were placed in an environment with saturated humidity conditions at 37 °C with 5% CO_2, and then sub-cultured in RPMI1640 medium containing 10% FBS, 50 U/mL penicillin and 100 g/mL streptomycin with medium changed at regular intervals every 2–3 d. Finally, cells exhibiting good growth at the logarithmic growth phase were selected for transfection.

2.6. Vector construction

According to the PDK1 (NC_000002.12) sequence information in Genebank, 3 interference sequences, si-PDK1–1, si-PDK1–2, si-PDK1–3 and NC (negative plasmids) were constructed, respectively (Table 1). DNA oligo was chemically prepared by Shanghai Genechem Co., Ltd. (Shanghai, China), inserted into plasmid containing the reporter gene cGFP marker and Neomycin resistance gene for construction of siRNA recombinant plasmid. The recombinant plasmid was then transformed into a competent *Escherichia coli* strain DH5α cell (Dalian Takara Co., Ltd., Dalian, Liaoning, China). Several single colonies were selected in the culturing process of a small number of bacteria. After the recombinant plasmid had been successfully constructed, the plasmid was extracted and stored at −20 °C for further experiments after the plasmid concentration had been measured. Prior to transfection, cells exhibiting good growth condition were seeded in a 6-well plate at the density of 5×10^3 cells. When cell coverage rate reached 50%~70%, the cells were transfected with the medium replaced with a fresh complete culture medium. The serum-and-antibiotic-free medium was added with transfection reagent Lipofectamine 2000 (Invitrogen Inc., Carlsbad, CA, USA) while the recombinant lentiviral plasmid or virus-containing supernatant infected by blank plasmid, was fully mixed, allowed to rest at room temperature for 20 min, dropped and then mixed again in a culture plate with cells. After 6 h of conventional culture, the medium was renewed with fresh complete culture medium. Reverse transcription quantitative polymerase chain reaction (RT-qPCR) methods were employed to determine the mRNA expression of PDK1 gene, while the plasmid exhibiting the best silencing effect was selected for subsequent transfection experimentation.

Table 1
siRNA sequence.

	Sequence (5′ – 3′)
si-PDK1-1	Sense: GGUUGUUGUUGGAGAAGCATT Anti-sense: UGCUUCUCCAACAACAACCTT
si-PDK1-2	sense: GGUCAGUAGUCUUGUAAUATT Anti-sense: UAUUACAAGACUACUGACCTT
si-PDK1-3	sense: CGAGAACAGCACACUUCAATT Anti-sense: UUGAAGUGUGCUGUUCUCGTT
NC	sense: UUCUCCGAACGUGUCACGUTT Anti-sense: ACGUGACACGUUCGGAGAATT

Note: Si-PDK1, silence-3-phosphoinositide-dependent protein kinase-1; NC, negative control.

2.7. Cell grouping and transfection

After conventional detachment, A498 and 786-O cells were collected and seeded into a 6-well culture plates and then assigned into 5 groups, respectively: blank group, NC group (transfected with empty plasmid negative control), si-PDK1–1 group (transfected with si-PDK1), IGF-1 group (added with activator IGF-1) and si-PDK1 + IGF-1 group (transfected with si-PDK1 and added with activator IGF-1). On the day before transfection, the culture medium was substituted with an antibiotic-free medium containing 10% FBS. In the event that the cells reached 70% ~ 80% confluence, transfection was performed in strict accordance with the instructions of Lipofectamine 2000 (Invitrogen Inc., Carlsbad, CA, USA). IGF-1 (20 ng/mL, 105–01, Shanghai Puxin Biological Technology Co., Ltd., Shanghai, China) was added in the IGF-1 group and the si-PDK1 + IGF-1 group 30 min before siRNA-PDK1 transfection [20]. After 4–6 h of transfection, the medium was replaced with medium containing with serum, with the green fluorescent protein detected in cells regarded to be an indication of successful transfection. At 48 h after transfection, cell transfection was observed under an inverted fluorescence microscope (CFM-500E/CFM-500Z, Shanghai Changfang Optical Instrument Co., Ltd., Shanghai, China), and the cells were collected for subsequent experiments.

2.8. RT-qPCR

Total RNA was extracted using ultra-pure RNA Extraction Kit (Dalian Takara Co., Ltd., Dalian, Liaoning, China) and primers of PDK1, PI3K, AKT, E-cadherin, N-cadherin, Vimentin, PCNA, Bcl-2, Bax and Caspase-3 were designed by primer design website and were synthesized by Dalian Takara Co., Ltd. (Dalian, China) (Table 2). Total RNA was reversely transcribed to cDNA using PrimeScript@RT reagent Kit (Dalian Takara Co., Ltd., Dalian, Liaoning, China) and kept at −20 °C for reserve. The reaction solution was taken to carry out the fluorescence quantitative PCR, and the experiment was carried out according to the instructions of SYBR Green RT-PCR reagent (Dalian Takara Co., Ltd., Dalian, Liaoning, China). Fluorescence quantitative PCR was conducted using an ABI PRISM®7300 (Prism ®7300, Shanghai Kunke Instrument Equipment Co., Ltd., Shanghai, China). The reaction conditions were as follows: pre-denaturation at 95 °C for 10 min and 40 cycles of denaturation at 95 °C for 15 s, annealing at 60 °C for 60 s,

Table 2
The primer sequence for RT-qPCR.

Gene	Sequence (5′ – 3′)
PDK1	Forward primer: TGAACTGACCTTGCCACAT
	Reverse primer: TGAAGCAGCACTGAACACG
PI3K	Forward primer: GCCCAGGCTTACTACAGAC
	Reverse primer: AAGTAGGGAGGCATCTCG
Akt	Forward primer: ACTCATTCCAGACCCACGAC
	Reverse primer: AGCCCGAATCGTTATCTT
E-cadherin	Forward primer: GAGTGCCAACTGGACCATTC
	Reverse primer: CACAGTCACACACGCTGACC
N-cadherin	Forward primer: TTTTGCCCCCAATCCTAAGA
	Reverse primer: CAGCGTTCCTGTTCCACTCAT
Vimentin	Forward primer: GACGGTTGAAACTAGAGATGG
	Reverse primer: GCTGGTAATATATTGCTGCA
PCNA	Forward primer: TCCCTTACGCAAGTCTCAGC
	Reverse primer: GTCCTTGAGTGCCTCCAACA
Bcl-2	Forward primer: ACGAGTGGGATGCGGGAGA
	Reverse primer: CCAGGAGAAATCAAACAGAGGC
Bax	Forward primer: GGATGCGTCCACCAAGAA
	Reverse primer: TGTCCCGAAGGAGGTTTATT
caspase-3	Forward primer: TTGTGGAATTGATGCGTGAT
	Reverse primer: TTCTGTTGCCACCTTTCG
GAPDH	Forward primer: TTCTTTTGCGTCGCCAGCCGA
	Reverse primer: GTGACCAGGCGCCCAATACGA

Note: RR-qPCR, reverse transcription quantitative polymerase chain reaction; PDK1, 3-phosphoinositide-dependent protein kinase-1; PCNA, proliferating cell nuclear antigen; PI3K, phosphoinositide 3-kinase; GAPDH, glyceraldehyde phosphate dehydrogenase; E-cadherin; epithelial cadherin; N-cadherin, neural cadherin; Bcl-2, B-cell lymphoma 2.

and extending at 72 °C for 1 min. Glyceraldehyde-3-phosphate dehydrogenase (GAPDH) gene was regarded as the internal reference, while the relative expression of the gene was calculated using the $2^{-\Delta\Delta CT}$ method [21]. The mRNA expression of PDK1 in normal tissues and mRNA expression of PDK1, PI3K, AKT, E-cadherin, N-cadherin, Vimentin, PCNA, Bcl-2, Bax and Caspase-3 in transfected cells were then calculated accordingly.

2.9. Western blot analysis

The lysis of RCC tissues and adjacent normal tissues was performed with protein lysate RIPA. After a 48 h period of transfection, the cells were detached with 0.1% trypsin with the total protein then extracted respectively. After centrifugation for 10 min at 10000 ×*g*, the supernatant was collected, and the total protein concentration was determined with the bicinchoninic acid (BCA) protein quantitative Kit (Beijing Cwbiotech Co., Ltd., Beijing, China) and preserved at −20 °C. The protein was then added with the loading buffer, boiled for 10 min in a water bath prior to centrifugation. The protein was loaded, and sodium dodecyl sulfate polyacrylamide gel electrophoresis (SDS-PAGE) was then conducted using a current of 25 mA for 1 h. Finally transfer to a polyvinylidene fluoride (PVDF) membrane at constant pressure of 60 V was performed. Membrane blockade was conducted with 5% skim milk powder and then incubated with the following primary antibodies for overnight reaction at 37 °C: rabbit anti-PDK1 (1: 1000; ab208187), p-PI3K(1: 1000; ab182651), PI3K(1: 1000; ab151549), p-AKT (1: 500; ab8933), AKT (1: 5000; ab64148), E-cadherin (1: 10000; ab40772), N-cadherin (1: 1000; ab76057), Vimentin (1: 2000; ab92547), PCNA (1: 1000; ab18197), Bcl-2 (1: 1000; ab32124), Bax (1: 2000; ab32503), caspase-3 (1: 500; ab13847), and GAPDH (1: 2500; ab9485) (Abcam, Cambridge, MA, USA). The membrane was incubated for 2 h at room temperature with the addition of horseradish peroxidase (HRP)-labeled secondary antibody goat anti-rabbit IgG (1: 5000, A21020, Wuhan Amyjet Scientific Co., Ltd., Wuhan, China). The enhanced chemiluminescence (ECL, 10001, Beijing Keyushenlan Biotechnology Co., Beijing, China) reaction solution was applied for developing purposes. Images were acquired using gel. The target protein expression was measured as the ratio of related genes and gray value of GAPDH (the internal reference) using Bandscan 5.0 gel imaging software.

2.10. 3-(4,5-dimethylthiazol-2-yl)-2,5-diphenyltetrazolium bromide (MTT) assay

The cells were seeded into a 96-well plate with 5×10^3 cells in each well (200 μL/well). Cells were transfected when the cell confluence reached 70% - 80%. Three duplicated wells were set for each group. MTT solution (20 μL, 5 g/L, GD-Y1317, Guduo biotechnology company, Shanghai, China) was added to each culture well at 24 h, 48 h, 72 h of transfection, respectively. After 4 h, with the supernatant solution discarded, 150 μL of dimethyl sulfoxide (DMSO, D5879-100ML, Sigma-Aldrich Chemical Company, St Louis, MO, USA) was added into each well. The 96-well plate was then continually vibrated at a low speed for 10 min. The optical density value (OD value) at 490 nm was measured using a microplate reader (DG5031, Ba Jiu Industrial Co., Ltd., Shanghai, China). The experiment was repeated 3 times.

2.11. Flow cytometry

After transfection for 48 h, the cells (1×10^6 cells/mL) at the logarithmic growth phase were centrifuged at 178 ×*g* for 5 min with culture solution removed. The cells were washed once with incubation buffer solution before centrifugation at 178 ×*g* for 5 min. According to the instructions of the Annexin-V-Fluorescein Isothiocyanate (FITC) cell apoptosis detection kit (K201–100, BioVision, Inc., San Francisco, CA, USA), Annexin-V-FITC/PI staining solution was prepared with Annexin-V-FITC, propidium iodide (PI), and N-2-Hydroxyethylpiperazine-N′-2-Ethanesulfonic Acid (HEPES buffer) at the proportion of 1: 2: 50. The cells were re-suspended with 100 μL labeled solution and incubated for 10 min at room temperature void of light. After centrifugation, the cells were washed with incubation buffer and incubated for 20 min at 4 °C with fluorescent solution SA-FLOUS (Origin Biosciences Inc., Nanjing, Jiangsu, China). Flow cytometry (CytoFLEX, CA92821, Beckman Coulter, Inc., Chaska, MN, USA) was applied in order to detect apoptosis by means of examining the FITC and PI fluorescence using the 525 nm and 620 nm bandpass filter at a 488 nm wavelength.

After transfection for 48 h, the cells in logarithmic growth phase were washed twice with PBS after which the supernatant was removed. The cells were then added with 70% precooled ethanol (1 mL), triturated evenly and fixed overnight at 4 °C. The cells were then washed twice with PBS and centrifuged at 178 ×*g* for 5 min. PBS solution (500 μL) was used to re-suspend the cells. PI (88,378, Sigma-Aldrich Chemical Company, St Louis, MO, USA) and RNase A (GE101–01, TransGen Biotech, Beijing, China) were added with the solution to the final concentration of 50 μg/mL, and the cells were bathed at 37 °C for

Table 3
Gene expression chip information of renal cell carcinoma.

Accession	Platform	Organism	Sample
GSE6344	GPL97	*Homo sapiens*	10 normal and 10 renal cell carcinoma tumors
GSE53757	GPL570	Homo sapiens	72 renal cell carcinoma tumor tissues and 72 normal kidneys
GSE14762	GPL6480	Homo sapiens	10 renal cell carcinoma tumor samples and 12 normal renal tissue
GSE781	GPL97	Homo sapiens	5 normal and 12 renal cell carcinoma kidney tissue

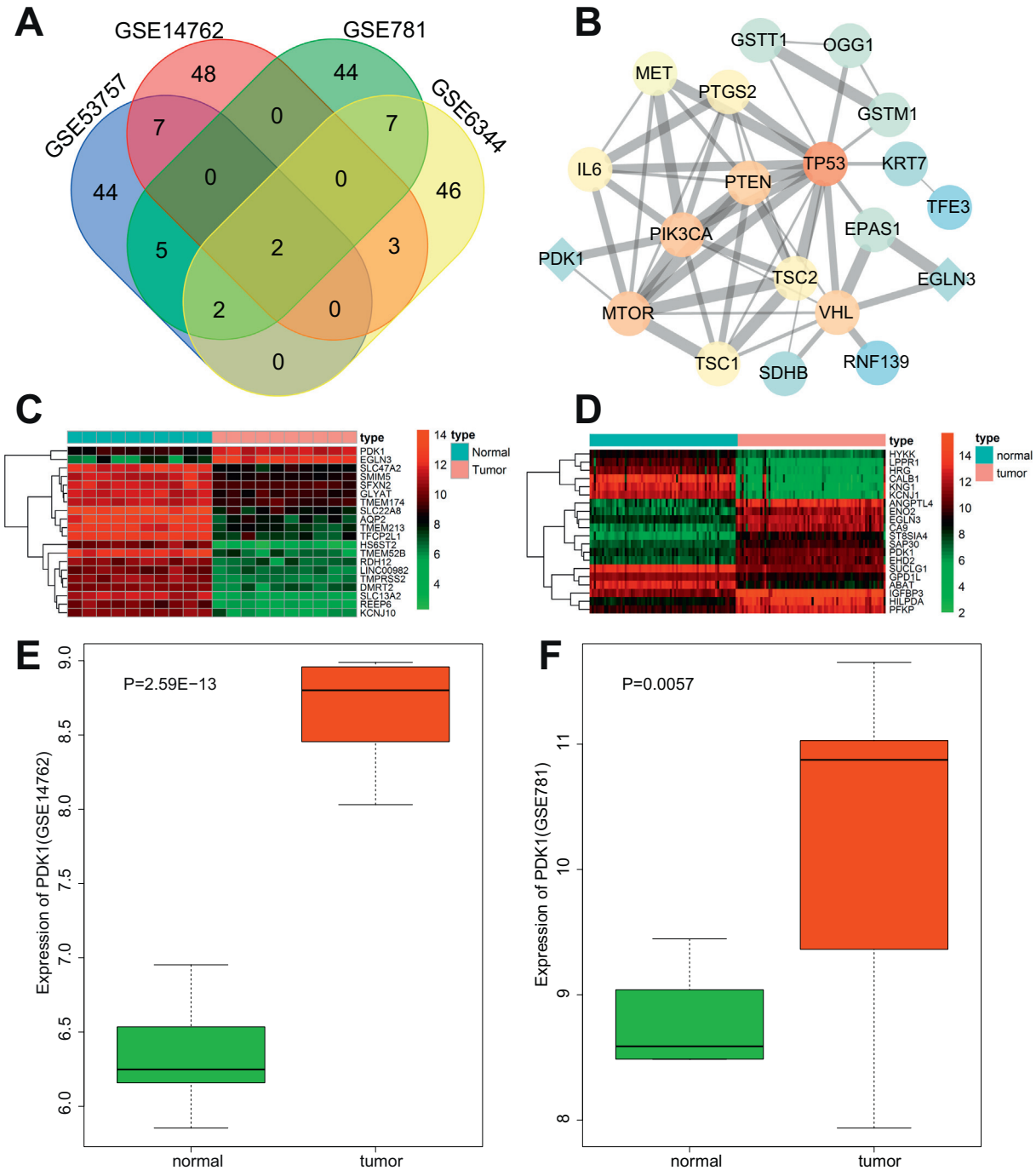

Fig. 1. GEO data analysis displays that PDK1 is associated with RCC. A, intersecting genes PDK1 and EGLN3 found in the top 60 DEGs of GSE6344, GSE53757, GSE14762 and GSE781 chips. B, a gene interaction network between PDK1 and EGLN3 and the known RCC-related genes. The rhomboid represented the DEGs, and the circle represented the known RCC-related gene. C and D, the expression heat map of the top 20 DEGs in GSE6344 and GSE53757 chips. The sample type is shown in the top color bar, and the sample number information is shown in Supplementary Table 1, and the vertical coordinate represents the DEGs. The histogram in the upper right referred to the color gradation, of which each rectangle corresponded to an expression value of a sample, with the red color representing high expression value and green color representing low expression value. E and F, expression change of PDK1 in GSE14762 and GSE781 chips. RCC, renal cell carcinoma; PDK1, 3-phosphoinositide-dependent protein kinase-1; EGLN, the egg-laying abnormal-9; DEGs differentially expressed genes. (For interpretation of the references to color in this figure legend, the reader is referred to the web version of this article.)

30 min. Cell cycle was measured using flow cytometry by recording the red fluorescence at an excitation wavelength of 488 nm.

2.12. Scratch test

The back of the six-well plate was marked with parallel lines at 0.5 cm intervals across the wells. The cells at the logarithmic growth phase exhibiting good growth conditions were conventionally detached and counted. The cells were then suspended with a complete culture medium, and evenly inoculated into a 6-well plate (5×10^5 cells/well). The next day, wounds were created using a pipette tip using a vertical orientation against the lines marked in the back of the plate. PBS solution was used to gently wash the cells in order to remove the floating cells, after which the cells were incubated with medium containing

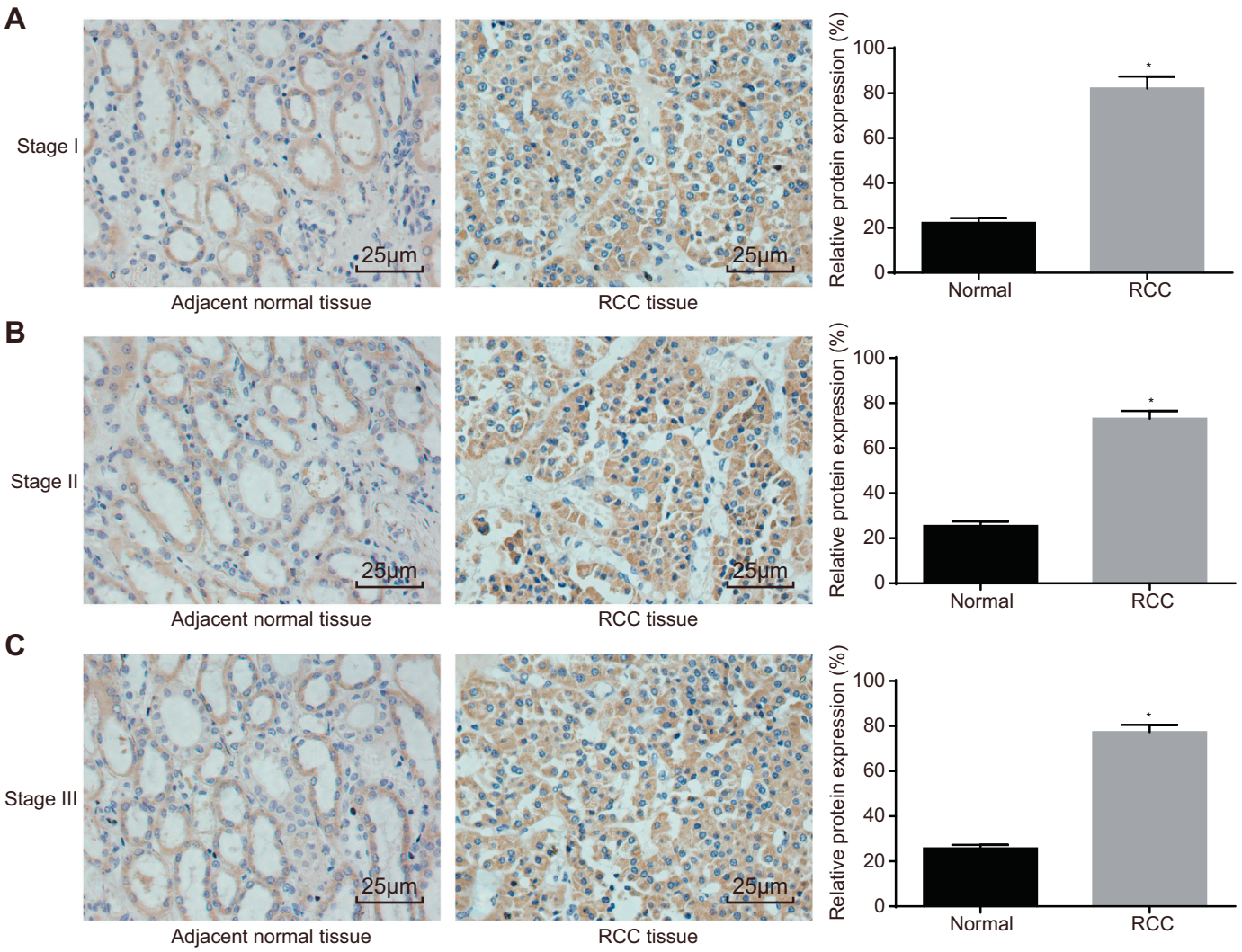

Fig. 2. Higher positive expression rate of PDK1 is found in RCC tissues. A, the positive expression of PDK1 in adjacent normal tissues and RCC tissues of patients at stage I (N = 18, scare bar = 25 um); B, the positive expression of PDK1 in adjacent normal tissues and RCC tissues of patients at stage II (N = 59, scare bar = 25 um); C, the positive expression of PDK1 in adjacent normal tissues and RCC tissues of patients at stage III (N = 35, scare bar = 25 um); The measurement data in figures were presented as mean ± standard deviation and analyzed by unpaired t-test. *, $p < 0.05$ *vs.* adjacent normal tissues; RCC, renal cell carcinoma; PDK1, 3-phosphoinositide-dependent protein kinase-1.

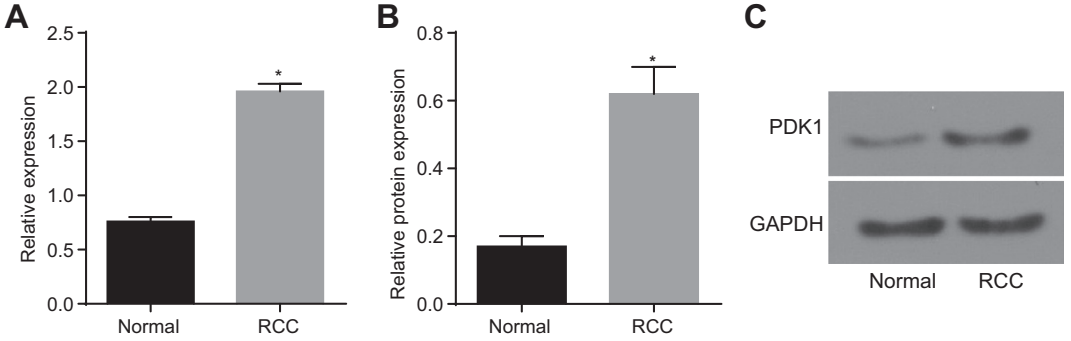

Fig. 3. The mRNA and protein expression of PDK1 is significantly higher in RCC tissues than that in adjacent normal tissues. A, the mRNA expression of PDK1 in normal and RCC tissues determined by RT-qPCR. B, the protein expressions of PDK1 in adjacent normal tissues and RCC tissues examined by western blot analysis; C, protein bands of PDK1 in adjacent normal tissues and RCC tissues (N = 35); *, $p < 0.05$ *vs.* adjacent normal tissues; The measurement data in figures were presented as mean ± standard deviation and analyzed by unpaired t-test. RCC, renal cell carcinoma; PDK1, 3-phosphoinositide-dependent protein kinase-1; RT-qPCR, reverse transcription quantitative polymerase chain reaction.

Table 4
The relationship between PDK1 and the clinicopathological factors of RCC cells.

Item	n	PDK1 protein expression				*p*
		High expression n (%)		Low expression n (%)		
Gender						0.540
Male	45	32	71.11%	13	28.89%	
Female	67	43	64.18%	24	35.82%	
Age						0.217
< 50	68	49	72.06%	19	27.94%	
≥ 50	44	26	59.09%	18	40.91%	
TNM stage						< 0.001
I/II	26	10	38.46%	16	61.54%	
III/IV	86	65	75.58%	21	24.42%	
Lymph node metastasis						< 0.001
Yes	62	52	83.87%	10	16.13%	
No	50	23	46.00%	27	54.00%	
Tumor diameter (cm)						0.426
< 5	54	34	62.96%	20	37.04%	
≥ 5	58	41	70.69%	17	29.31%	
WHO/ISUP grading						0.016
I	18	7	38.89%	11	61.11%	
II	59	41	69.49%	18	30.51%	
III	35	27	77.14%	8	22.86%	

Note: RCC, renal cell carcinoma; TNM, tumor node metastasis; PDK1, 3-phosphoinositide-dependent protein kinase-1.

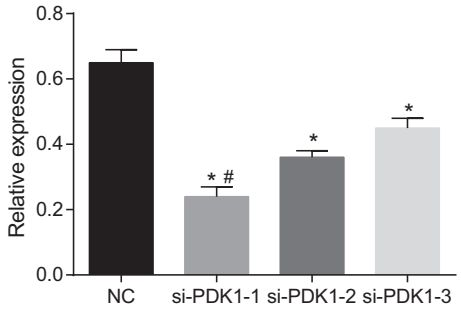

Fig. 4. si-PDK1–1 is determined to be the best silencing plasmid through comparison among 786-O cells transfected by NC, si-PDK1–1, si-PDK1–2, and si-PDK1–3; *, $p < 0.05$ *vs.* the NC group; #, $p < 0.05$ *vs.* the si-PDK1–2, and si-PDK1–3 groups; NC, negative control; si-PDK1, silence-3-phosphoinositide-dependent protein kinase-1.

0.2% bovine serum albumin (BSA) at 37 °C in a 5% CO_2 incubator. At the 0 h and 24 h time points, the cells were observed and photographed under an inverted microscope. Finally, the migration distance between the scratches on the cells was measured and recorded.

2.13. Transwell assay

Transwell chambers (3413, Beijing Uni Biological Technology Co., Ltd., Beijing, China) with filter membrane of 8 μm aperture were selected. Matrigel (Becton, Dickinson and Company, Franklin Lakes, NJ, USA) was melted at 2 °C–8 °C overnight. Matrigel (100 μL) was added with the 300 μL serum-free culture medium and mixed evenly. The diluted Matrigel was added to the apical chamber, which was covered using a polycarbonate film at 37 °C for 30 min until the Matrigel was confirmed to have solidified. The cells collected from each group were made into 2.5×10^6 cells/mL cell suspension. Cell suspension (200 μL) was added to the basolateral chamber, and 500 μL culture medium containing 10% FBS was also added to the basolateral chamber used as a chemotactic factor. After incubation at 37 °C for 48 h, tumor cells that failed to invade the stroma were removed with using cotton swabs. The cells were then fixed by 4% paraformaldehyde for 30 min, stained with 0.1% crystal violet. Five high magnification fields were randomly selected, with the OD value at 570 nm measured and the average value then obtained.

2.14. Statistical analysis

Statistical analyses were conducted using SPSS 21.0 software (IBM Corp. Armonk, NY, USA). The experiments were conducted three times in each group. Measurement data were expressed as mean ± standard deviation. Comparisons between two groups were analyzed using unpaired *t*-test. One-way analysis of variance (ANOVA) was used for comparing data among multiple groups. Enumeration data were expressed as percentages, while comparisons between two groups were performed using a chi-square test. $p < 0.05$ was indicative of statistical significance.

3. Results

3.1. PDK1 and the PI3K/Akt pathway are related to RCC

DEGs with $|\text{LogFoldChange}| > 2.0$ and $p < 0.05$ were screened based on RCC expression chips GSE6344, GSE53757, GSE14762 and GSE781 in GEO database (Table 3). The top 60 DEGs of each chip were compared and then used to construct a Venn map (Fig. 1A), with the two intersecting genes, PDK1 and EGLN3 detected. RCC-related genes were checked in DisGeNET and the following 20 genes were selected as known RCC-related genes: VHL, TFE3, TP53, TSC1, PIK3CA, OGG1, HNF1A, RNF139, EPAS1, TSC2, PTEN, MET, GSTM1, SDHB, GSTT1, IL6, MTOR, KRT7, BIRC7, and PTGS2. The String tool then was used to analyze the interaction between the intersecting DEGs as well as the known RCC-related genes, in order to construct a gene interaction network (Fig. 1B). A key observation revealed that in the gene interaction network, PDK1 was associated with two RCC-related genes, PIK3CA and MTOR, and the related pathways of those three genes were analyzed in KEGG website to found that PDK1, PIK3CA and MTOR were all involved in the PI3K-Akt pathway (map04151: http://www.kegg.jp/kegg-bin/highlight_pathway?scale=1.0&map=map04151). Numerous studies have suggested that the activation of P13K-Akt pathway is related to RCC [22,23]. The heat map of top 20 DEGs in GSE6344 (Fig. 1C) and GSE53757 (Fig. 1D) was constructed, and demonstrated that the expression of PDK1 were significantly increased in RCC tissues, while abnormally high expressions were detected among the RCC tissues in GSE14762 (Fig. 1E) and GSE781 (Fig. 1F) chips.

3.2. Higher PDK1 expression rate is determined in RCC tissues

In accordance with the immunohistochemistry results, PDK1 was determined to possess varying degrees of expression in both the RCC tissues and adjacent normal tissues. PDK1 was found to be mainly expressed in the cytoplasm and cell membrane of the tumor cells, with the positive expression represented by yellow or brown granules (Fig. 2A). The positive expression rate of PDK1 was determined to be (22.22 ± 2.13)% in adjacent normal tissues and (82.12 ± 5.32)% in RCC tissues of patients at stage I, (25.42 ± 2.05)% and (73.05 ± 3.45)%, respectively of patients at stage II, and (25.71 ± 1.56)% and (77.29 ± 3.26)%, respectively of patients at stage III (all $p < 0.05$) (Fig. 2B). These findings demonstrated that RCC tissues exhibited a higher positive rate of PDK1.

3.3. The higher expression of PDK1 is found in RCC tissues

RT-qPCR and Western blot analysis methods were employed in order to detect the mRNA and protein expression of PDK1 in RCC tissues and adjacent normal tissues. The results (Fig. 3A–C) demonstrated that compared with the adjacent normal tissues, the RCC tissues

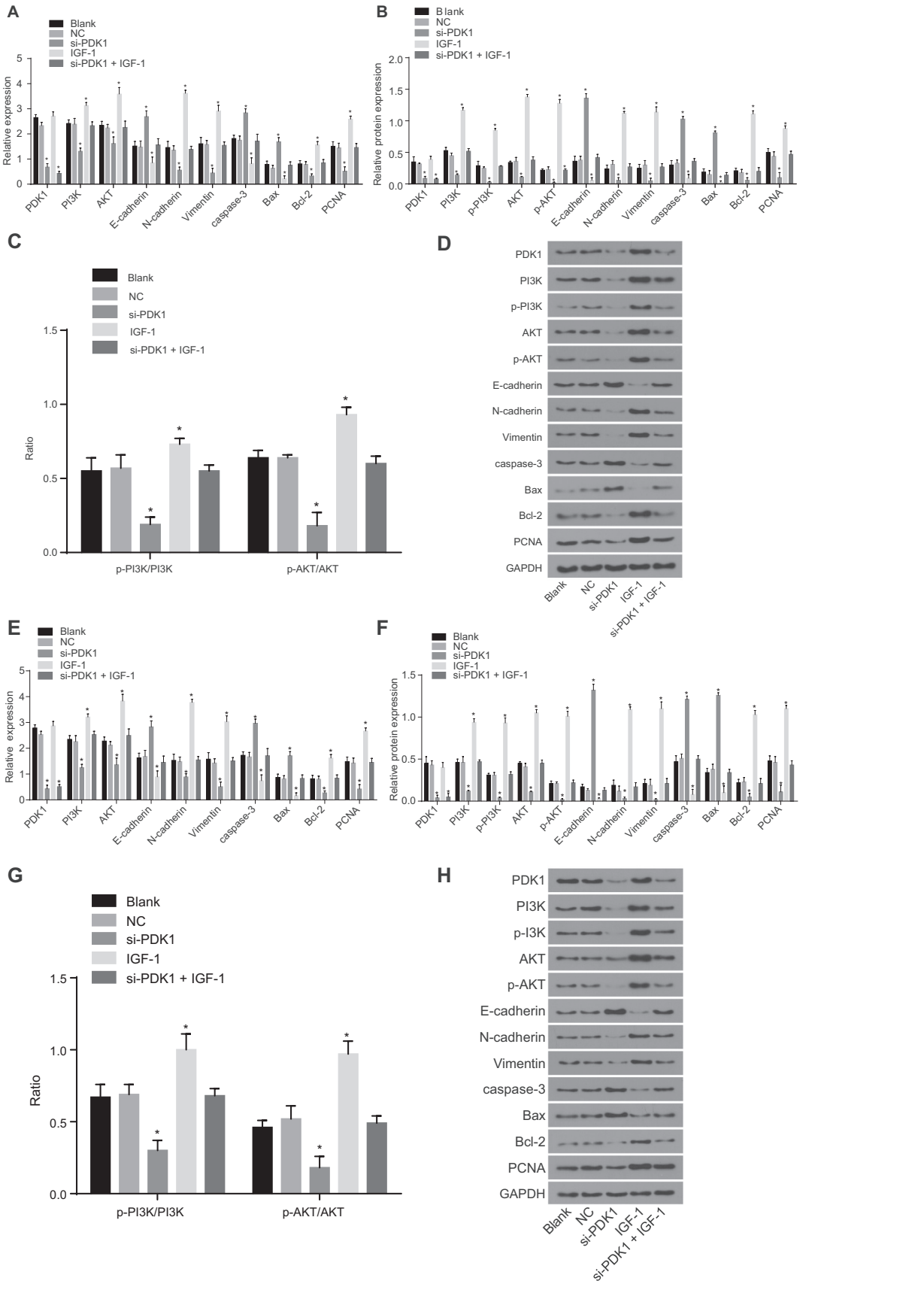

(caption on next page)

Fig. 5. Downregulated PDK1 regulates the PI3K-PDK1-Akt pathway. A, mRNA expression of related factors in A498 cells examined by RT-qPCR; B, protein expression of related factors in A498 cells examined by western blot analysis; C, the protein ratio of A498 cells; D, the protein bands of related factors in A498 cells; E, mRNA expression of related factors in 786-O cells examined by RT-qPCR; F, protein expression of related factors in 786-O cells examined by western blot analysis; G, the protein ratio of 786-O cells; H, the protein bands of related factors in 786-O cells. The p-P13K antibody (1: 1000, ab182651, Abcam, Cambridge, UK) and p-AKT antibody (1: 500, ab8933; Abcam, Cambridge, UK) were used in experiment and the protein expression of target gene was presented as the ratio of gray value of related genes to internal reference GAPDH, which is determined using Bandscan 5.0 gel imaging software. *, $p < 0.05$ *vs.* the blank and NC groups. NC, negative control; The measurement data in figures were presented as sample mean ± standard deviation and analyzed by one-way analysis of variance; the experiment was repeated 3 times. RT-qPCR, reverse transcription quantitative polymerase chain reaction, PI3K, phosphoinositide 3-kinase; PDK1, 3-phosphoinositide-dependent protein kinase-1; GAPDH, glyceraldehyde-3-phosphate dehydrogenase.

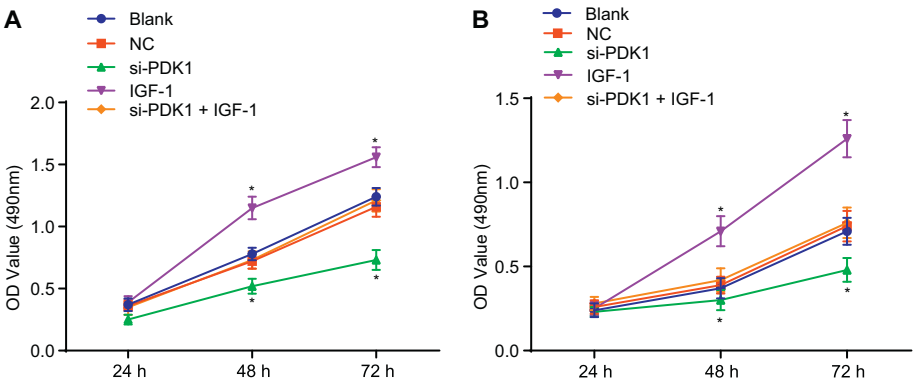

Fig. 6. RCC cell proliferation was inhibited by si-PDK1. A, the OD value of A498 cells at 24 h, 48 h and 72 h; B, the OD value of 786-O cells at 24 h, 48 h and 72 h. *, $p < 0.05$ *vs.* the blank and NC groups; the measurement data in figures were presented as sample mean ± standard deviation and analyzed by repeated measurement analysis of variance; the experiment was repeated 3 times. RCC, renal cell carcinoma; Si-PDK1, silence-3-phosphoinositide-dependent protein kinase-1; IGF-1, Insulin-like growth factor-1; NC, negative control.

displayed significantly elevated mRNA and protein expression of PDK1 ($p < 0.05$).

3.4. PDK1 is closely related with TNM stage, lymph node metastasis and WHO/ISUP grading of RCC

Among the 112 cases of RCC tissues, there were 75 cases with high expressions of PDK1, while 37 cases exhibited low expressions. The protein expression of PDK1 was determined to be closely related to the TNM stage, lymph node metastasis and WHO/ISUP grading (all $p < 0.05$). There was no significant correlation detected between the protein expression of PDK1 and gender, age and tumor diameter of patients with RCC (all $p > 0.05$) (Table 4).

3.5. Effect of PDK1 siRNAs on expression of its mRNA

The mRNA expressions of PDK1 in the NC group, the si-PDK1-1 group, the si-PDK1-2 group and the si-PDK1-3 group were examined, the results of which revealed (Fig. 4): the mRNA expression of PDK1 gene in 786-O cells in the si-PDK1-1 group, the si-PDK1-2 group and the si-PDK1-3 group was lower than that of the NC group ($p < 0.05$), while the mRNA expression of the PDK1 gene in the si-PDK1-1 group was the lowest ($p < 0.05$). The obtained result demonstrated that si-PDK1-1 was the plasmid with the best silencing effect and therefore selected for subsequent experiments.

3.6. Silencing of PDK1 inhibits the activation of PI3K-PDK1-Akt pathway and the EMT of RCC cells, while promotes RCC cell apoptosis

In order to determine the levels of PDK1, PI3K-PDK1-Akt pathway-related factors, apoptosis-related factors and EMT-related factors in A498 and 786-O RCC cells, RT-qPCR and Western blot analysis methods were employed. The results (Fig. 5) displayed there to be no significant difference relating to the reactivity between A498 and 786-O cells in addition to no significant difference detected regarding the expression of PDK1, PI3K, AKT, N-cadherin, Vimentin, E-cadherin, Bax, caspase-3, Bcl-2 and PCNA as well as the extent of p-PI3K and p-AKT between the blank group and the NC group ($p > 0.05$). Comparisons between the blank and NC groups, the si-PDK1 group displayed markedly reduced mRNA and protein expression of PDK1, PI3K, AKT, N-cadherin, Vimentin, Bcl-2, and PCNA, while significantly increased mRNA and protein expression of E-cadherin, Bax, and caspase-3, greatly decreased extent of p-PI3K and p-AKT as well as a decreased ratio of p-PI3K/PI3K as well as a decreased p-AKT/AKT ratio (all $p < 0.05$). However, the IGF-1 group exhibited significantly elevated mRNA and protein expression of PI3K, AKT, N-cadherin, Vimentin, Bcl-2, PCNA but reduced E-cadherin, Bax, caspase-3, increased extent of p-PI3K and p-AKT as well as elevated ratio of p-PI3K/PI3K, and p-AKT/AKT (all $p < 0.05$), while with no remarkable difference found in the mRNA and protein expression of PDK1 ($p > 0.05$). Compared with the blank and NC groups, in the si-PDK1 + IGF-1 group, the mRNA and protein expression of PDK1 was greatly reduced ($p < 0.05$), the ratio of p-PI3K/PI3K and p-AKT/AKT remained unchanged, with no significant difference detected in the other genes ($p > 0.05$). The results revealed that PDK1 gene silencing could inhibit the activation of the PI3K-PDK1-Akt pathway and the EMT of RCC cells, while promoting RCC cell apoptosis.

3.7. PDK1 gene silencing inhibits RCC cell proliferation

MTT assay was conducted in order to observe cell proliferation at 24 h, 48 h, and 72 h. The results (Fig. 6) indicated there was no significant difference regarding proliferative ability between the A498 and 786-O cells in addition to know detected notable difference between each group at the 24 h time point ($p > 0.05$). Compared with the blank group and the NC group, the si-PDK1 group demonstrated decreased cellular proliferative ability at the 48 h and 72 h time points ($p < 0.05$), while the IGF-1 group illustrated increased cellular proliferation ability at the 48 h and 72 h time points ($p < 0.05$). No significant difference in relation to the proliferation abilities of the cells in the si-PDK1 + IGF-1 group was detected ($p > 0.05$). The results suggested that the inhibition of PDK1 could inhibit the proliferation of RCC cells.

3.8. PDK1 gene silencing causes RCC cell cycle arrest

Flow cytometry was applied to examine cell cycle, the results (Fig. 7A-B) of which revealed there to be no significant difference regarding cell cycle distribution between the A498 and 786-O cells in addition to no statistical significance detected during each phase between the blank group, the NC group and the si-PDK1 + IGF-1 group

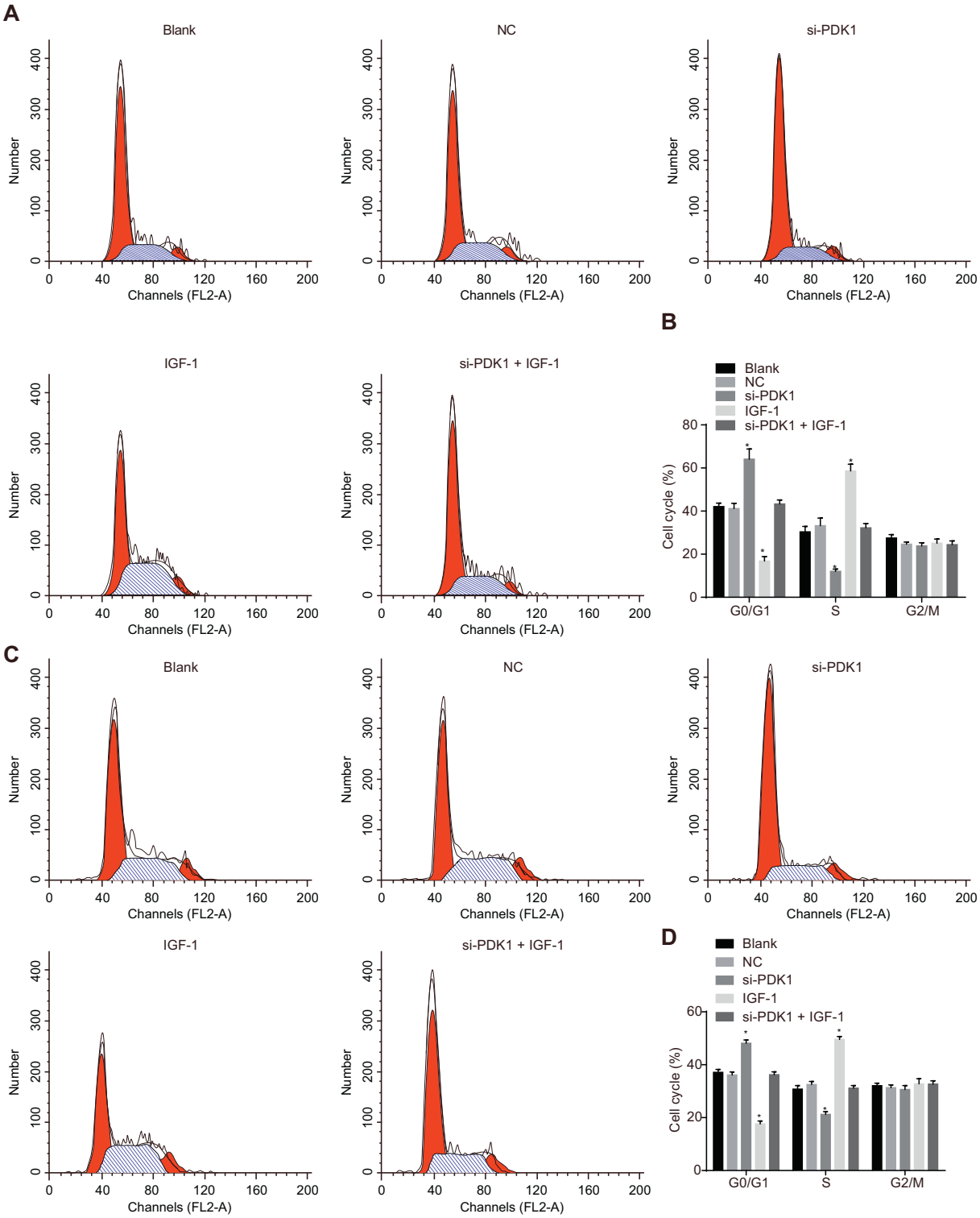

Fig. 7. Effect of si-PDK1 on cell cycle in RCC cells, and PDK1 gene silencing causes RCC cell cycle arrest. A, cell cycle analysis produced by flow cytometry in A498 cells after transfection; B, percentages of A498 cells in G0/G1, S and G2/M phase; C, cell cycle analysis produced by flow cytometry in 786-O cells after transfection; D, percentages of 786-O cells in G0/G1, S and G2/M phase; *, $p < 0.05$ *vs.* the blank and NC groups. The measurement data in figures were presented as sample mean ± standard deviation and analyzed by repeated measurement analysis of variance; the experiment was repeated 3 times. Si-PDK1, silence-3-phosphoinositide-dependent protein kinase-1; IGF-1, Insulin-like growth factor-1; NC, negative control; RCC, renal cell carcinoma.

($p > 0.05$). Compared with the blank group and the NC group, the si-PDK1 group displayed promoted cell proportion at the G0/G1 phase, and suppressed cell proportion at the S phase ($p < 0.05$) while the IGF-1 group exhibited decreased cell proportion at the G0/G1 phase and increased cell proportion at the S phase ($p < 0.05$). There was no notable difference among the cells at the G2 phase between all the groups ($p > 0.05$). These results indicated that silenced PDK1 could arrest cells at the G0/G1 phase.

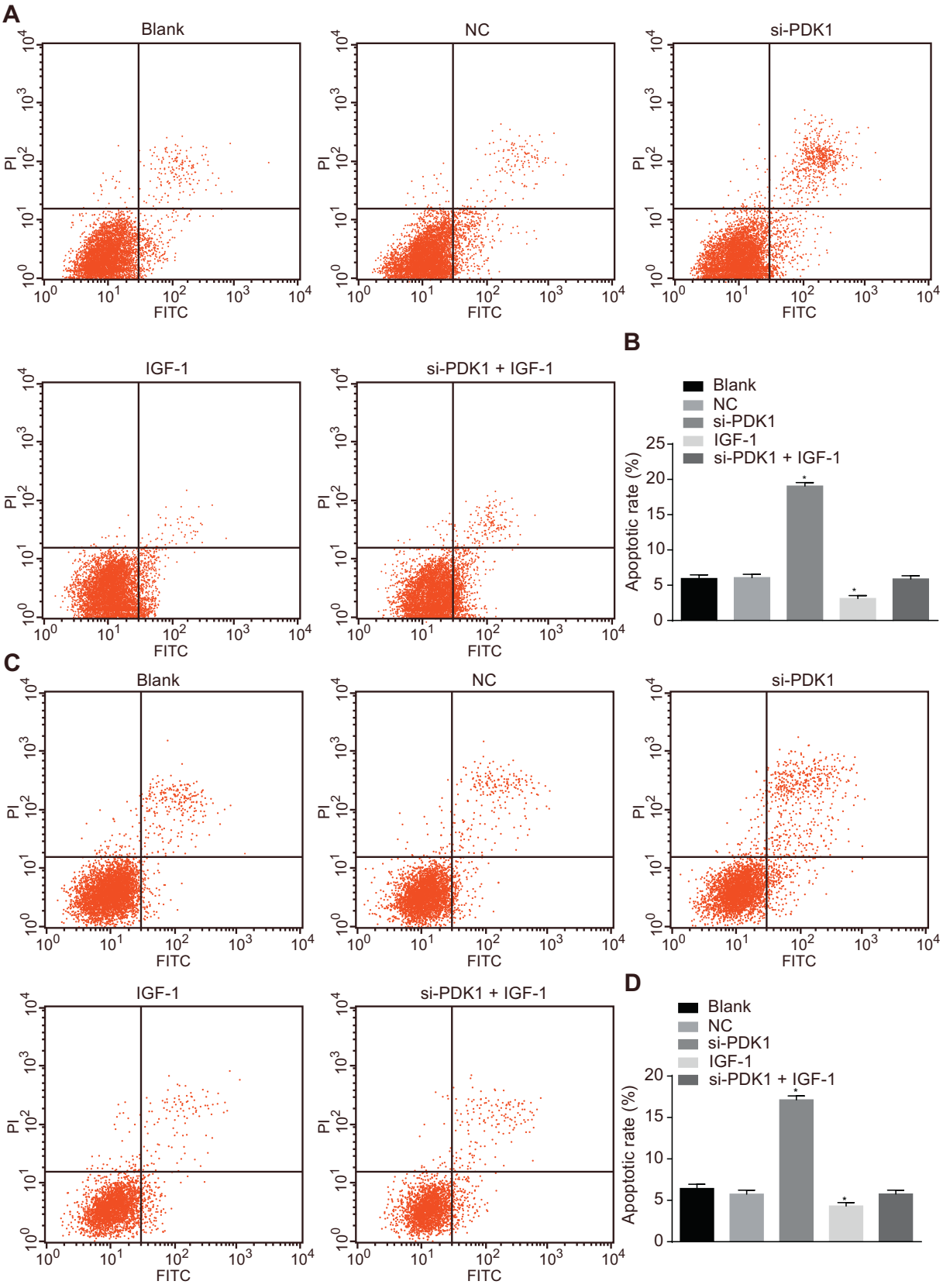

Fig. 8. PDK1 gene silencing suppresses RCC cell apoptosis. A, the apoptosis of A498 cells in each group; B, the apoptosis rate of A498 cells in each group; C, the apoptosis of 786-O cells in each group; D, the apoptosis rate of 786-O cells in each group; *, $p < 0.05$ *vs.* the blank and NC groups; the measurement data in figures were presented as sample mean ± standard deviation and analyzed by one-way analysis of variance; the experiment was repeated 3 times. Si-PDK1, silence-3-phosphoinositide-dependent protein kinase-1; RCC, renal cell carcinoma; NC, negative control.

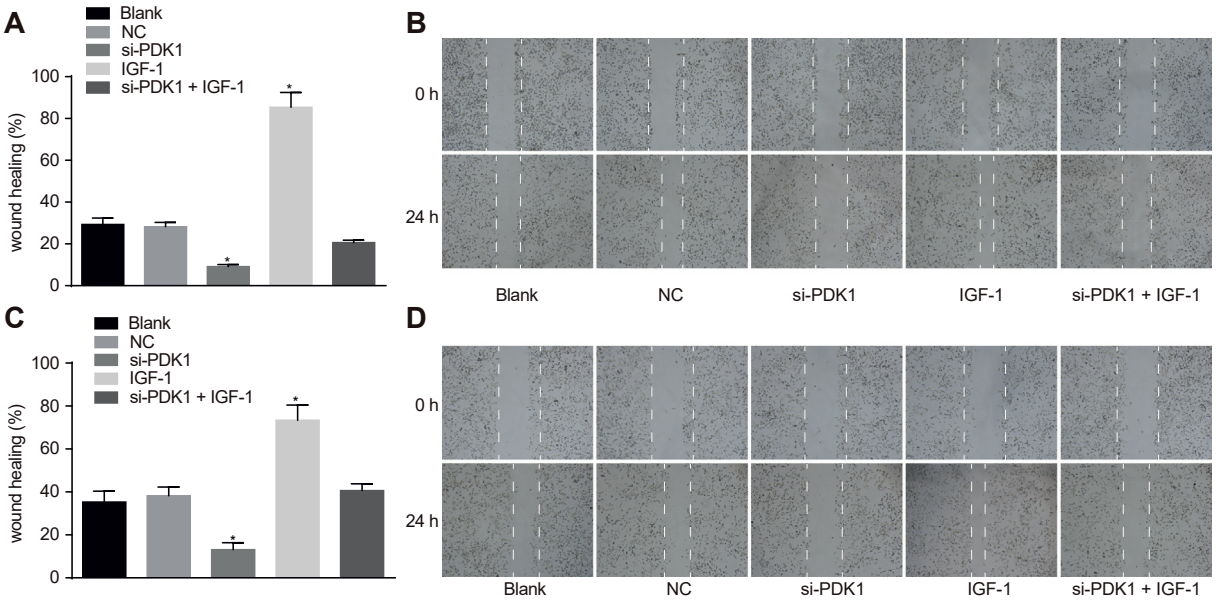

Fig. 9. IGF-1 promotes the cell migration while si-PDK1 prevents the cell migration. A-B, the migration of A498 cells in each group; C-D, the migration of 786-O cells in each group; *, $p < 0.05$ *vs.* the blank and NC groups. The measurement data in figures were presented as sample mean ± standard deviation and analyzed by one-way analysis of variance; the experiment was repeated 3 times. Si-PDK1, silence-3-phosphoinositide-dependent protein kinase-1; IGF-1, Insulin-like growth factor-1; NC, negative control.

3.9. PDK1 gene silencing promotes cell apoptosis

RCC cell apoptosis was also analyzed by means of flow cytometry, the results of which (Fig. 8A-B) indicated there to be no difference in terms of cell apoptosis between the A498 and 786-O cells. Compared with the blank group and the NC group, the si-PDK1 group exhibited an upward trend in cell apoptosis ($p < 0.05$), while the IGF-1 group displayed a decreasing trend regarding cell apoptosis ($p < 0.05$). There was no significant difference regarding the apoptosis rate between the blank group and the NC group ($p > 0.05$). The apoptosis rate in the si-PDK1 + IGF-1 group was found not to be significantly different from that in the blank and NC groups ($p > 0.05$). Based on our observations we concluded that suppressed PDK1 enhanced the apoptosis of RCC cells.

3.10. PDK1 gene silencing lowers RCC cell migration

Scratch test methods were employed to help detect cell migration, the results (Fig. 9A-B) of which revealed there to be no significant difference between the cell migration of the A498 and 786-O cells. After 24 h, compared with the blank group and the NC group, the IGF-1 group demonstrated significantly increased cell migration distance ($p < 0.05$), indicating enhanced migration ability, while the si-PDK1 group had significantly decreased cell migration distance ($p < 0.05$), indicating reduced migration ability. No remarkable difference in terms of cell migration distance in the si-PDK1 + IGF-1 group was detected when compared with the blank and NC groups ($p < 0.05$). Based on the above result, we concluded that, PDK1 gene silencing can inhibit RCC cell migration.

3.11. PDK1 gene silencing suppresses invasive ability of RCC cells

Transwell assay was adopted to detect the cell invasion, and the results (Fig. 10 A-B) showed that there was no significant difference in cell invasion between A498 and 786-O cells and no significant difference was found among the blank group, the NC group and the si-PDK1 + IGF-1 group. Compared with the blank group and the NC group, the IGF-1 group show displayed markedly up-regulated cell density with stronger invasion ability, while the si-PDK1 group displayed greatly down-regulated cell density with decreased invasion ability (all $p < 0.05$). Consequently, PDK1 gene silencing was determined to significantly reduce the invasive ability of the RCC cells.

4. Discussion

As a highly invasive disease ranking 13th among all known tumors RCC [24] is widely known to exhibit intrinsic insensitivity to chemotherapy and radiotherapy, with surgery remaining the only remedial tactic against RCC, highlighting the urgent need for novel RCC treatment methods [25]. PDK-1 functions as an essential signaling member in the PI3K pathway, playing a central role in RCC [26,27]. The aim of the current study was to elucidate the mechanism by which PDK1 is associated to RCC with the involvement of PI3K-PDK1-Akt pathway. Our observations revealed that interfering with the expression of PDK1 gene could inhibit the activation of the PI3K-PDK1-Akt pathway, ultimately inhibiting the EMT of RCC, which resulted in the prevention of proliferation and promotion of RCC cell apoptosis.

Initially, the results of this study demonstrated that si-PDK1 up-regulated the protein and mRNA expression of E-cadherin while it down-regulated the protein and mRNA expression of vimentin, and subsequently inhibited the EMT. A previous study suggested that EMT is an orderly, polygenic biological process that functions as a significant role in tumor cell chemoresistance, invasion, and metastasis [28]. Studies have shown that inducing EMT and JunB, PDK1 promotes cell invasion and proliferation, and metastasis in gallbladder cancer [29]. Feng et al. asserted that vascular remodeling was regulated and EMT was promoted in cardiac development by PDK1 [30]. All the above findings were strongly consistent with the findings of our study.

A key observation of the current study revealed that silenced PDK1 decreased the extent of p-PI3K and p-AKT and decreased ratio of p-PI3K/PI3K and the ratio of p-AKT/AKT, suggesting that the activation of the PI3K-PDK1-Akt pathway was inhibited by si-PDK1 through prohibiting the phosphorylation of PI3K and AKT. Studies have indicated that the refined and balanced regulation of the PDK1-Akt pathway is an important factor for cardiovascular development, as either a less activity or higher intensity of the Akt pathway elevated developmental

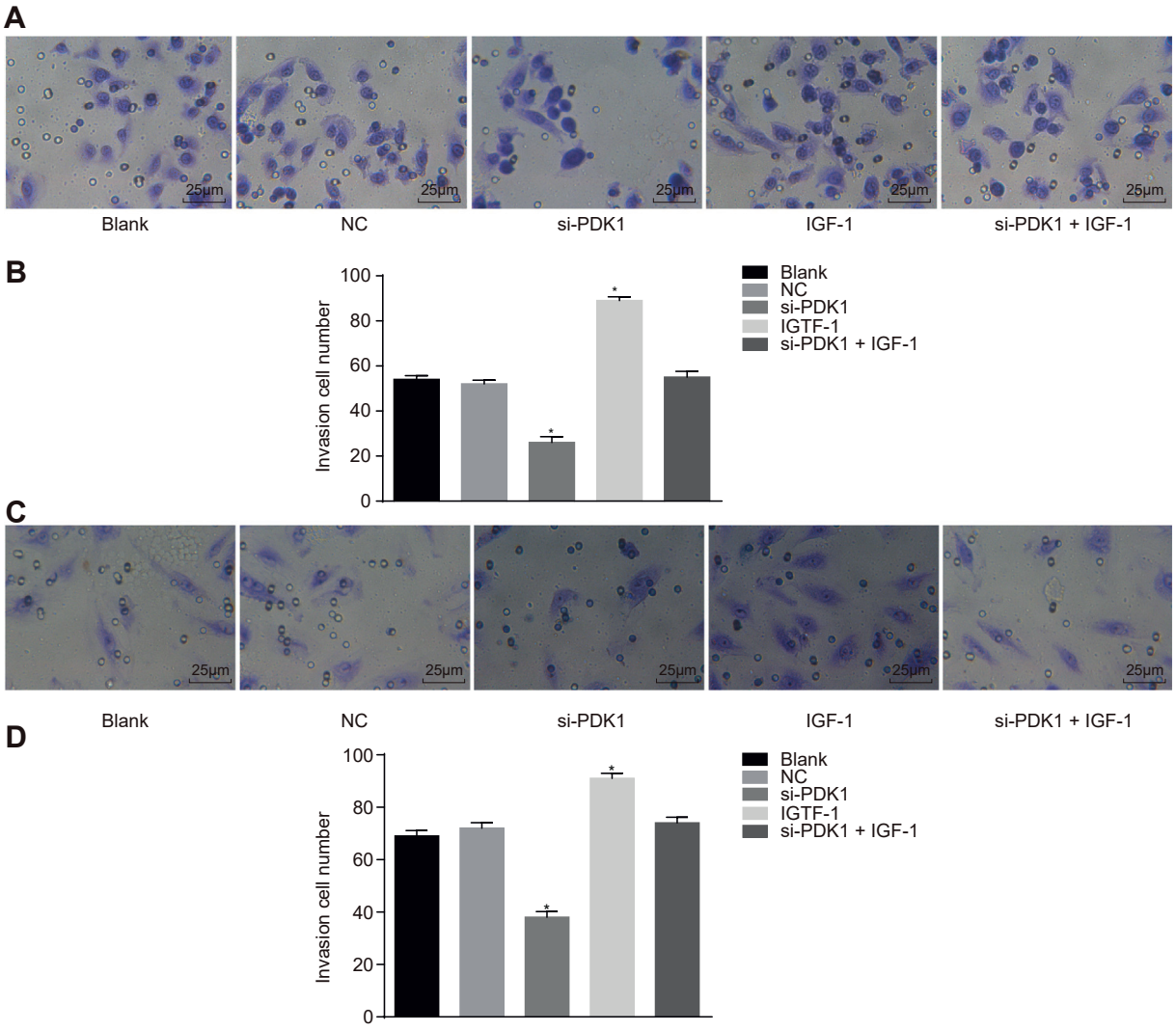

Fig. 10. Si-PDK1 inhibits cell invasion of RCC cells. A, the invasive A498 cells in each group; B, the invasive cell number of A498 cells in each group; C, the invasive 786-O cells in each group; B, the invasive cell number of 786-O cells in each group; *, $p < 0.05$ *vs.* the blank and NC groups. The measurement data in figures were presented as sample mean ± standard deviation and analyzed by one-way analysis of variance; the experiment was repeated 3 times. Si-PDK1, silence-3-phosphoinositide-dependent protein kinase-1; NC, negative control.

abnormalities [30]. Xu et al. suggested that with the help of PDK1, Akt is activated through the phosphorylation of Thr308 of Akt, and the activated Akt phosphorylates numerous substrates, further affecting numbers of physiological and cellular processes, such as cell cycle, cellular growth, survival, apoptosis, and migration [28]. Moreover, current literature has suggested that the dephosphorylation of PDK-1 is related to the induction of apoptosis which further negatively influences the new cell proliferation rate [31]. The investigation conducted by Vanhaesebroeck et al. revealed that PDK1 exists in a phosphorylated, active configuration under basal conditions and is refractive to extra phosphorylation and activation upon cell promotion with agonists which activated PI3K [32].

In addition, we arrived at the conclusion based on our findings that RCC cells, PDK1 was highly expressed and the PI3K-PDK1-Akt pathway was activated. Furthermore, si-PDK1 could prohibit the activation of the PI3K-PDK1-Akt pathway and further promote the apoptosis of RCC cells and suppress the RCC cell proliferation, invasion, and migration. In line with our study, Baumunk et al. also found evidence of high expressions PDK1 in RCC [27]. Reports have indicated that the PI3K/Akt pathway plays an important role in regulating cell proliferation and maintaining the biological characteristics of malignant cells [28]. A previous study suggested that suppressed PDK1/Akt kinase could inhibit the cell proliferation and promote apoptosis in oophoroma cells [33]. IGF-1 is a recognized anti-apoptotic and pro-survival factor and the PI3K/Akt pathway is involved in cell survival induced by IGF-1, which is in accordance with our own experiment results [9]. The apoptosis of myeloid leukemia cells has been implicated in the upregulation of Bax and caspase-3 expression, which is strongly related to the inactivation of the PI3K/Akt pathway [34].

5. Conclusions

The key observations of the current study suggest that siRNA targeting PDK1 in RCC cells inhibited the EMT, and promoted the RCC cell apoptosis and inhibited proliferation, invasion, and migration through suppressing the activation of the PI3K-PDK1-Akt pathway (Fig. 11). PDK1 may serve as a potential novel therapeutic target in RCC. There were certain limitations faced by our study including the number of histological samples or the use of methods, indicating that further studies on the prognostic significance of PDK1 are required in the future to further verify our findings.

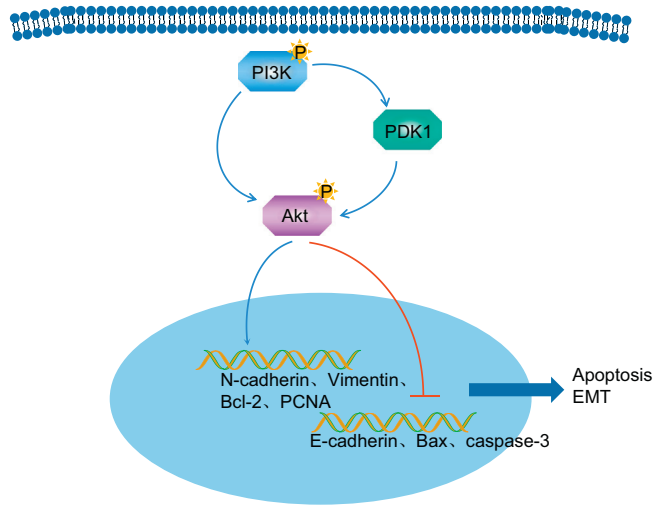

Fig. 11. Map of molecular mechanisms involved in PDK1 regulation in proliferation, apoptosis and epithelial mesenchymal transition of renal cell carcinoma cells. PDK1 is upregulated with dysregulated PI3K-PDK1-Akt pathway in renal cell carcinoma. With the treatment of PDK1 gene silencing, the apoptosis and epithelial mesenchymal transition of renal cell carcinoma cells were inhibited by reduced expression of N-cadherin, Vimentin, Bcl-2, and PCNA, while promoted expression of E-cadherin, Bax, and caspase-3 through the suppression of the PI3K-PDK1-Akt pathway. PDK1, 3-phosphoinositide-dependent protein kinase-1; PI3K, phosphatidylinositol-3-kinases; Bcl-2, B-cell lymphoma 2; PCNA, proliferating cell nuclear antigen; E-cadherin; epithelial cadherin; N-cadherin, neural cadherin.

Competing interests

The authors have declared that no competing interests exist.

Acknowledgments

We would like to give our sincere appreciation to the reviewers for their helpful comments on this article.

Appendix A. Supplementary data

Supplementary data to this article can be found online at https://doi.org/10.1016/j.cellsig.2018.11.016.

References

[1] P. Chen, et al., miR-216a-5p acts as an oncogene in renal cell carcinoma, Exp Ther Med. 15 (4) (2018) 4039–4046.
[2] P. Chen, et al., Tumor suppressor microRNA-136-5p regulates the cellular function of renal cell carcinoma, Oncol. Lett. 15 (4) (2018) 5995–6002.
[3] A.M. Franzen, et al., Metastases to both Parotid Glands six and twelve years after Resection of Renal Cell Carcinoma, Case Rep. Med. 2018 (2018) 7301727.
[4] J. Masannat, et al., betaArrestin2 Mediates Renal Cell Carcinoma Tumor Growth, Sci. Rep. 8 (1) (2018) 4879.
[5] Y.L. Ma, F. Chen, J. Shi, Rhein inhibits malignant phenotypes of human renal cell carcinoma by impacting on MAPK/NF-kappaB signaling pathways, Onco Targets Ther. 11 (2018) 1385–1394.
[6] M. Terasaki, et al., Glycine and succinic acid are effective indicators of the suppression of epithelial-mesenchymal transition by fucoxanthinol in colorectal cancer stem-like cells, Oncol. Rep. 40 (1) (2018) 414–424.
[7] P.A. Gagliardi, L. di Blasio, L. Primo, PDK1: a signaling hub for cell migration and tumor invasion, Biochim. Biophys. Acta 1856 (2) (2015) 178–188.
[8] U. Kilic, et al., Particular phosphorylation of PI3K/Akt on Thr308 via PDK-1 and PTEN mediates melatonin's neuroprotective activity after focal cerebral ischemia in mice, Redox Biol. 12 (2017) 657–665.
[9] C. Kim, S. Park, IGF-1 protects SH-SY5Y cells against MPP(+)-induced apoptosis via PI3K/PDK-1/Akt pathway, Endocr Connect. 7 (3) (2018) 443–455.
[10] K. Thillai, et al., Deciphering the link between PI3K and PAK: an opportunity to target key pathways in pancreatic cancer? Oncotarget 8 (8) (2017) 14173–14191.
[11] S. Chen, et al., Tetrandrine inhibits migration and invasion of human renal cell carcinoma by regulating Akt/NF-kappaB/MMP-9 signaling, PLoS ONE 12 (3) (2017) e0173725.
[12] S. Shimobaba, et al., Claudin-18 inhibits cell proliferation and motility mediated by inhibition of phosphorylation of PDK1 and Akt in human lung adenocarcinoma A549 cells, Biochim. Biophys. Acta 1863 (6 Pt A) (2016) 1170–1178.
[13] R.A. Irizarry, et al., Exploration, normalization, and summaries of high density oligonucleotide array probe level data, Biostatistics 4 (2) (2003) 249–264.
[14] J. Pinero, et al., DisGeNET: a discovery platform for the dynamical exploration of human diseases and their genes, Database (Oxford) 2015 (2015) (bav028).
[15] P. Shannon, et al., Cytoscape: a software environment for integrated models of biomolecular interaction networks, Genome Res. 13 (11) (2003) 2498–2504.
[16] J. Dagher, et al., Clear cell renal cell carcinoma: validation of World Health Organization/International Society of Urological Pathology grading, Histopathology 71 (6) (2017) 918–925.
[17] M. May, et al., Prognostic and discriminative power of the 7th TNM classification for patients with surgically treated papillary renal cell carcinoma: results of a multi-institutional validation study (CORONA subtype project), Scand J. Urol. 51 (4) (2017) 269–276.
[18] B. Cai, et al., CMTM5 inhibits renal cancer cell growth through inducing cell-cycle arrest and apoptosis, Oncol. Lett. 14 (2) (2017) 1536–1542.
[19] E. Ertekin, et al., Role of Contrast Enhancement and Corrected Attenuation Values of Renal Tumors in predicting Renal Cell Carcinoma (RCC) Subtypes: Protocol for a Triphasic Multi-Slice Computed Tomography (CT) Procedure, Pol. J. Radiol. 82 (2017) 384–391.
[20] L. Zhang, et al., The Effects of IGF-1 on TNF-alpha-Treated DRG Neurons by Modulating ATF3 and GAP-43 Expression via PI3K/Akt/S6K Signaling Pathway, Neurochem. Res. 42 (5) (2017) 1403–1421.
[21] S.M. Ayuk, H. Abrahamse, N.N. Houreld, The role of photobiomodulation on gene expression of cell adhesion molecules in diabetic wounded fibroblasts in vitro, J. Photochem. Photobiol. B 161 (2016) 368–374.
[22] H. Guo, et al., The PI3K/AKT Pathway and Renal Cell Carcinoma, J. Genet. Genomics. 42 (7) (2015) 343–353.
[23] Y. Zhu, et al., Klotho suppresses tumor progression via inhibiting PI3K/Akt/GSK3beta/Snail signaling in renal cell carcinoma, Cancer Sci. 104 (6) (2013) 663–671.
[24] X. Wang, et al., Involvement of erbB4 and tumor marker genes in renal carcinoma regulatory network, Saudi J. Biol. Sci. 24 (8) (2017) 1787–1791.
[25] S. Zhang, Y. Ren, J. Qiu, Dauricine inhibits viability and induces cell cycle arrest and apoptosis via inhibiting the PI3K/Akt signaling pathway in renal cell carcinoma cells, Mol. Med. Rep. 17 (5) (2018) 7403–7408.
[26] B. Chaurasia, et al., Phosphoinositide-dependent kinase 1 provides negative feedback inhibition to Toll-like receptor-mediated NF-kappaB activation in macrophages, Mol. Cell. Biol. 30 (17) (2010) 4354–4366.
[27] D. Baumunk, et al., Expression parameters of the metabolic pathway genes pyruvate dehydrogenase kinase-1 (PDK-1) and DJ-1/PARK7 in renal cell carcinoma (RCC), World J. Urol. 31 (5) (2013) 1191–1196.
[28] W. Xu, Z. Yang, N. Lu, A new role for the PI3K/Akt signaling pathway in the epithelial-mesenchymal transition, Cell Adhes. Migr. 9 (4) (2015) 317–324.
[29] S. Lian, et al., PDK1 induces JunB, EMT, cell migration and invasion in human gallbladder cancer, Oncotarget 6 (30) (2015) 29076–29086.
[30] Q. Feng, et al., PDK1 regulates vascular remodeling and promotes epithelial-mesenchymal transition in cardiac development, Mol. Cell. Biol. 30 (14) (2010) 3711–3721.
[31] C.C. King, M. Obonyo, Helicobacter pylori modulates host cell survival regulation through the serine-threonine kinase, 3-phosphoinositide dependent kinase 1 (PDK-1), BMC Microbiol. 15 (2015) 222.
[32] B. Vanhaesebroeck, D.R. Alessi, The PI3K-PDK1 connection: more than just a road to PKB, Biochem. J. 346 (Pt 3) (2000) 561–576.
[33] J.H. Choi, et al., Potential inhibition of PDK1/Akt signaling by phenothiazines suppresses cancer cell proliferation and survival, Ann. N. Y. Acad. Sci. 1138 (2008) 393–403.
[34] J.J. Liu, et al., Inactivation of PI3k/Akt signaling pathway and activation of caspase-3 are involved in tanshinone I-induced apoptosis in myeloid leukemia cells in vitro, Ann. Hematol. 89 (11) (2010) 1089–1097.